Tapered Dual-Plane Compact Electromagnetic Bandgap Microstrip Filter Structures

Shao Ying Huang, *Student Member, IEEE,* and Yee Hui Lee, *Member, IEEE*

***Abstract*—In this paper, the designs of two novel tapered dual-plane compact electromagnetic bandgap (C-EBG) microstrip filter structures are presented. With the dual-plane configuration, the proposed structure displays an ultrawide stopband with high attenuation within a small circuit area. Chebyshev distribution is adopted to eliminate ripples in the passband caused by the periodicity of the EBG structure. This gives rise to a compact EBG structure that exhibits excellent transmission and rejection characteristics in the passband and the stopband, respectively. The proposed structures are implemented and the measurement results are found to be in good agreement with the simulation results, verifying the excellent stopband and passband performance obtained using the proposed configuration. These novel structures are easy to fabricate and are promising structures that have wide applications for compact and high performance circuit component designs in microwave circuits.**

***Index Terms*—Bandstop filters, dual-plane, electromagnetic bandgap (EBG) structures, low sidelobe array theory, microstrip filters, tapering functions, tapering techniques.**

I. Introduction

ELECTROMAGNETIC bandgap (EBG) structure has been a term widely accepted nowadays to name the artificial periodic structures that prohibit the propagation of electromagnetic waves at microwave or millimeter wave frequencies. The three-dimensional (3-D) artificial periodic bandgap structure was introduced at optical frequencies [1]–[3] and known as photonic bandgap (PBG) structure. Due to the scalability of the periodic structure, relevant research work has progressed into the field of microwave, millimeter wave, and infrared.

The unique feature of EBG structures is the existence of the bandgap where electromagnetic waves are not allowed to propagate. It has been widely applied as the substrate of planar microwave circuits such as patch antennas to suppress the surface waves [4], [5] and power amplifiers to reduce the harmonics [6]. The planar EBG structure was introduced in [7] where planar periodic elements are etched in the ground plane. It has the advantage of ease of fabrication and yet capable of maintaining a similar control on the wave propagation in the structure to that in the EBG structure with 3-D periodic elements. The only drawback of planar structures is that they are not able to prohibit the wave propagation in the entire 3-D space. Nevertheless, planar EBG structures are compatible with microstrip circuits thus making them attractive as microstrip filters.

Manuscript received December 9, 2004; revised May 26, 2005.

The authors are with the School of Electrical and Electronic Engineering, Nanyang Technological University, 639798 Singapore (e-mail: syhuang@pmail.ntu.edu.sgl; eyhlee@ntu.edu.sg).

Digital Object Identifier 10.1109/TMTT.2005.854212

A microstrip line with an array of patches etched in the ground plane exhibits a prominent bandgap in the transmission along the conducting line [7]. Due to the high confinement of electromagnetic waves around the transmission line, the well-known one-dimensional (1-D) EBG microstrip reflector was proposed [8] where a single column of etched periodic elements below the line is sufficient to obtain a bandgap when the Bragg reflection condition is satisfied. A bandgap can be obtained in the EBG microstrip structure when the geometry of the etched patch is changed or when the periodic elements are introduced in the microstrip line [9], [10]. Defected ground structure (DGS) has a defect with unique geometry and is able to exhibit an attenuation pole even with a single unit [11].

Several approaches have been taken to enhance the stopband performance of 1-D planar EBG microstrip Bragg reflectors while maintaining a reasonable ripple level in the passband and keeping a small physical size. For example, in order to design a high performance bandstop filter that exhibits a wide stopband with high attenuation in a relatively small physical area, a meander 1-D EBG microstrip structure was proposed [12]. In [13], a compact EBG bandstop filter structure with a wide stopband was proposed by combining a 1-D periodic DGS and a modulated microstrip line. This structure is able to introduce an increase in the bandwidth of the stopband while maintaining a small ripple level in the lower passband.

A novel tapered dual-plane compact EBG (C-EBG) microstrip filter structure has been introduced in [14]. Due to the dual-plane configuration and the adopted tapering technique, the proposed structure exhibits superior passband and stopband characteristics. In this paper, the characteristics of the novel unique dual-plane configuration of the proposed design are studied in detail. A comprehensive study on the tapering techniques in the application for 1-D EBG microstrip structures is presented including formulas and a comparison of the effects of different tapering techniques. In Section II, the two single-plane EBG structures that are used to construct the proposed C-EBG structures are studied. The relative location of the single-plane EBG structures and its effects on the performance of the C-EBG structure are examined and analyzed. A comparison between the performances of the proposed structure and its associated single-plane EBG structures is included. In Section III, a systematical study on tapering techniques is presented. In Section IV, two novel tapered dual-plane C-EBG microstrip filter structures with significant elimination of ripples are proposed by adopting the Chebyshev distribution. The proposed C-EBG structures were fabricated and tested. Experimental results are presented in the same section.

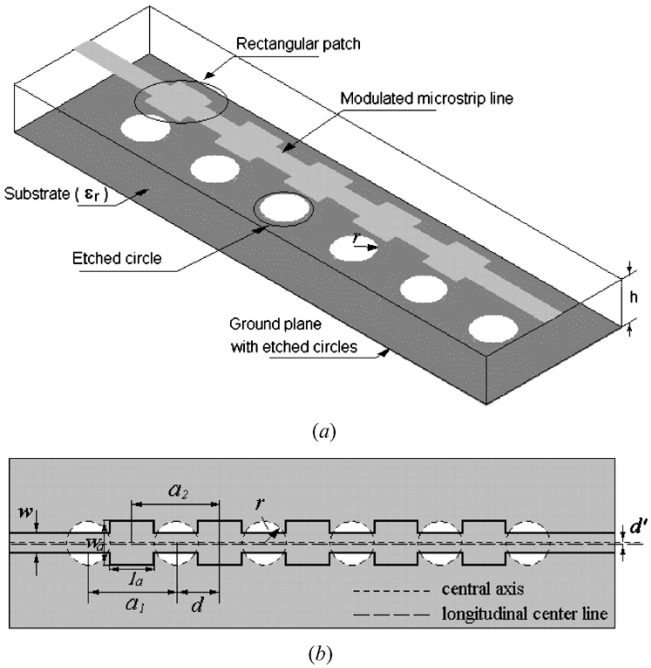

Fig. 1. Schematic of the proposed dual-plane C-EBG microstrip structure. (a) 3-D view. (b) Top view.

II. Dual-Plane Compact EBG (C-EBG) Microstrip Filter Structure

Fig. 1(a) and (b) shows the 3-D schematic and top view of the proposed dual-plane compact EBG (C-EBG) microstrip structure, respectively. As can be seen in Fig. 1(a), the proposed structure consists of the two single-plane EBG structures. One of which is a ground plane with etched circles, while the other is a modulated microstrip line. Between these two planes, there is a dielectric material with a relative permittivity of ε_r and a thickness of h.

A. Single-Plane EBG Microstrip Structures

The single-plane EBG microstrip structure consisting of a single column of circles with uniform dimension etched in the ground plane below a simple straight transmission line is a typical 1-D planar EBG microstrip structure. By etching circles in the ground plane, the coupling between the transmission line and the ground plane is reduced and therefore additional inductance is seen by the microstrip line. This 1-D planar EBG structure exhibits a bandgap when the Bragg reflection condition is satisfied [8].

The distance between the centers of two adjacent circles defines the period of the structure a_1. According to the Bragg reflection condition, the period a_1 is approximated by the following expression:

$$\beta \cdot a_1 = \pi \tag{1}$$

where β is the guided wavenumber in the substrate material and is described by the following equation:

$$\beta = \frac{2\pi}{\lambda_g} \tag{2}$$

where λ_g is the guided wavelength and is given by

$$\lambda_g = \frac{c}{f_0 \cdot \sqrt{\epsilon_{\text{eff}}}} \tag{3}$$

where f_0 is the center frequency of the stopband, ϵ_{eff} is the effective permittivity of the substrate material, and c is the speed of light in free space. From (1) and (2), the period a_1 equals half of the guided wavelength λ_g as expressed by the following equation:

$$a_1 = \frac{\lambda_g}{2}. \tag{4}$$

The radius of the circle is represented by r. The ratio of r and a_1 (r/a_1) is called filling factor which is used to indicate the relative size of the EBG cell to the period of the structure. In the case where there is no overlap between any two adjacent circles, it ranges from 0 to 0.5. For an EBG structure with uniform distribution, Radisic *et al.* [7] have shown that a large filling factor introduces a wide and deep stopband while increasing the ripple level in the passband. In [7], the optimal value of r/a_1 is found to be 0.25 where a good compromise between the stopband and passband performance can be obtained.

The other single-plane EBG structure used is the modulated microstrip line with no etched holes in the ground plane, as can be seen on the top of the proposed C-EBG structure (Fig. 1). It is a modulated microstrip line with rectangular patches periodically inserted in it. A prominent stopband can be obtained in the transmission of this microstrip line.

In Fig. 1(b), the length and width of the patch is represented by l_a and w_a, respectively. The width of the microstrip line is w. In this EBG structure, the variation range of w_a is expressed as

$$w_a > w. \tag{5}$$

With a width that is larger than the width of the microstrip line, the EBG unit increases the coupling between the microstrip line and the ground plane, and accordingly increases the capacitance. Moreover, these patches guarantee the power-handling capability of the transmission line. The structure also satisfies the Bragg reflection condition and therefore, the period of the structure a_2 can also be determined by (4).

B. Dual-Plane C-EBG Microstrip Structure Design

The proposed C-EBG structure is designed by superposing the two single-plane EBG structures mentioned above to obtain a dual-plane configuration, resulting in a structure shown in Fig. 1. The center frequency of the EBG structure on each plane is identical. According to (3) and (4), a_1 equals a_2. As can be seen in Fig. 1(b), with the dual-plane arrangement, the proposed C-EBG structure is able to increase the variation of reactance in the longitudinal direction due to the additional equivalent inductance and capacitance introduced by the etched circles and the inserted patches, respectively. Therefore, its stopband performance can be enhanced. In this C-EBG structure, the relative location between the two single-plane EBG structures is the key factor in deciding the enhancement of the stopband performance.

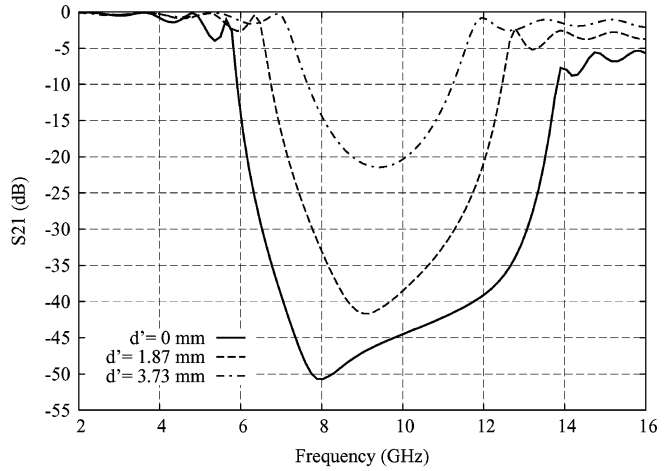

Fig. 2. Simulated S_{21} parameters of the dual-plane C-EBG structures with a varying d' and $d = 5.18$ mm.

C. Effects of Relative Location Between the Two Single-Plane EBG Structures

Due to the dual-plane configuration, the relative location of the single-plane EBG structure on each plane (d' and d) has significant effects on the performance of the proposed structure. The transversal alignment offset d' and the longitudinal offset d are illustrated in Fig. 1(b). d' is defined as the distance between the central axis of the circles and the longitudinal center line of the modulated microstrip line in the transversal direction. d is defined as the short distance between the centers of the adjacent etched circle and rectangular patch in the longitudinal direction. It ranges from 0 to $a_1/2(\text{or } a_2/2)$, and periodically repeats anywhere else. d' and d indicate the relative location between the two single-plane EBG structures in the transversal and the longitudinal direction, respectively.

The method-of-moments (MOM)-based software, *Zeland IE3D* is used to simulate the proposed dual-plane C-EBG microstrip structure (Fig. 1). The simulation model consists of a microstrip line with five inserted square patches and a ground plane with six etched circles. The substrate used is Taconic with a dielectric constant (ε_r) of 2.43 and a thickness (h) of 30 mils. To operate in the X-band range, the center frequency of each single-plane EBG structure is set to be 10 GHz. Therefore, according to the Bragg reflection condition, the period of the EBG structure a_1 and a_2 are both 10.35 mm. The width of the microstrip line w is set to 2.29 mm, corresponding to a characteristics impedance of 50 Ω at 10 GHz. The filling factor (r/a_1) is set to its optimal value of 0.25. Using this optimal filling factor, the radius of the circle is determined to be 2.59 mm. The length and the width of the inserted patch in the microstrip line l_a and w_a are both fixed to 5 mm.

Fig. 2 shows the simulated S_{21} parameters of the C-EBG structures with a fixed $d = 5.18$ mm and a varying $d' = [0 \text{ mm}, 1.87 \text{ mm}, 3.73 \text{ mm}]$. As can be seen in Fig. 2, as d' increases, the 10-dB stopband bandwidth reduces from 7.91 to 5.70 to 3.55 GHz. The C-EBG structure with circles etched exactly below the microstrip line ($d' = 0$ mm) shows the largest stopband bandwidth. The performances of these three C-EBG structures are tabulated in Table I. As shown in the table, a decrease in d' gives rise to an increase in both the bandwidth and the attenuation within the stopband. However, as d' decreases, the ripple level in both the higher and the lower passband increases. It is also observed that due to the higher insertion loss at high frequencies, the ripple level in the higher passband is always larger than that in the lower passband.

TABLE I
SIMULATED PERFORMANCES OF DUAL-PLANE C-EBG STRUCTURES.

C-EBG Structure	10 dB Bandwidth	Attenuation (dB)	Ripple Level (dB)	
			Lower	Higher
$d' = 3.73$ mm, $d = 5.18$ mm	3.55 GHz	21.46	1.64	2.57
$d' = 1.87$ mm, $d = 5.18$ mm	5.70 GHz	41.67	2.64	5.20
$d' = 0$ mm, $d = 5.18$ mm	7.91 GHz	50.72	3.97	8.80
$d' = 0$ mm, $d = 2.59$ mm	5.55 GHz	45.58	3.80	8.87

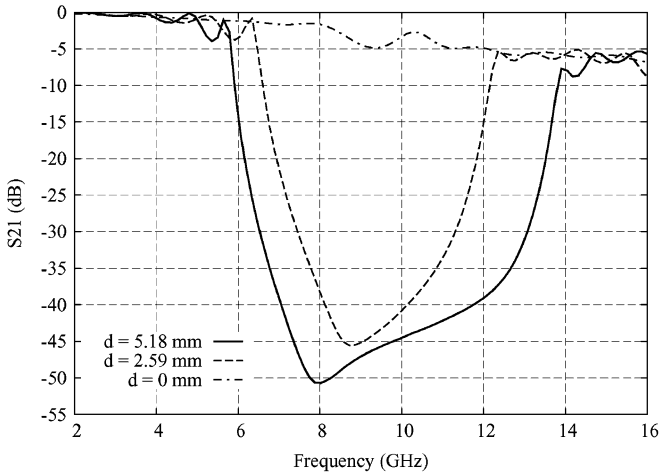

Fig. 3. Simulated S_{21} parameters of the dual-plane C-EBG structures with a varying d and $d' = 0$ mm.

The results reveal that in the proposed dual-plane C-EBG structure, an increase in the transversal alignment offset d' degrades the stopband performance significantly with only a slight improvement in the passband performance. This is because the equivalent inductance introduced by the etched circles diminishes with an increase in d' due to the high confinement of fields around the microstrip line. $d' = 0$ mm is the optimal location to significantly enhance the stopband performance because it gives the largest variation of equivalent reactance in the C-EBG structure.

Fig. 3 depicts the simulated S_{21} parameters of the dual-plane C-EBG structures with a fixed $d' = 0$ mm and a varying $d = [5.18 \text{ mm}, 2.59 \text{ mm}, 0 \text{ mm}]$. When $d = 5.18$ mm, there is no overlap between the etched circle in the ground plane and the inserted patch in the microstrip line; when $d = 2.59$ mm, the etched circle partially overlaps the inserted patch; and when $d = 0$ mm, they almost totally overlap each other. As can be seen in the figure, when $d = 0$ mm, no stopband is observed since the additional capacitive effect introduced by the inserted square patches cancels the inductive effect introduced by the circles of similar size etched in the ground plane. The performances of the two C-EBG structures with a stopband are included in Table I. As shown in the table, when d is decreased from 5.18 to 2.59 mm, the stopband performance of the C-EBG structure is

degraded in terms of bandwidth and attenuation. Its ripple level in the higher passband increases while its performance in the lower passband is slightly improved.

The results obtained imply that the longitudinal offset d considerably affects the stopband performance of the proposed dual-plane C-EBG microstrip structure while its effect on the passband performance is minor. The bandwidth and attenuation of the stopband decrease with a decreasing d. This is because the reduction in the longitudinal offset introduces a section of microstrip line without the inductive effect, and an overlap between the etched circle and the inserted patch where the inductive effect introduced by the etched circle cancels out the capacitive effect introduced by the inserted patch. It equivalently decreases the variation of reactance along the transmission line, thus degrades the stopband performance. From the analysis, the optimal configuration of the C-EBG structure happens when there is no overlap between the EBG units on the two different planes.

In the design of the proposed dual-plane C-EBG structure, a large variation of equivalent reactance can only be obtained when both the longitudinal offset d and the dimension of EBG units on both planes are properly determined. In the C-EBG structure with d set to $a_1/2$ (or $a_2/2$) and a fixed radius of the circle r ($r/a_1 = 0.25$), the length of the inserted patch l_a is determined by the following expression:

$$l_a \leq a_1 - 2r \tag{6}$$

to avoid any overlap between the etched circle and the inserted patch. The variation of equivalent reactance along the microstrip line is proportional to l_a when w_a is fixed. Thus, when $l_a = a_1 - 2r$, the variation is maximized and a good stopband performance can be obtained. With $d' = 0$ mm, $d = 5.18$ mm, and $l_a = 5$ mm, the proposed dual-plane C-EBG structure satisfies the condition in (6). It has the optimal relative location of the two single-plane EBG structures and a $l_a = a_1 - 2r$. Therefore, it shows a highly attenuated stopband with a large bandwidth.

D. Comparison Between Single-Plane and Dual-Plane EBG Structures

With the dimension of the EBG units set previously, the two single-plane EBG structures; the straight microstrip line with six circles etched in the ground plane (SP-six-circle); the modulated microstrip line on a smooth ground plane (SP-five-patch); and the proposed dual-plane C-EBG structure with the optimal relative location are simulated and compared. Fig. 4 shows the simulated S_{21} parameters of all three structures. As can be seen from the figure, SP-five-patch EBG structure has a 10-dB bandwidth of 3.27 GHz with an attenuation of 20.17 dB, a ripple level of 1.60 dB in the lower passband, and a ripple level of 2.55 dB in the higher passband. The bandwidth performance of this structure is poor, however, its ripple level performance is very promising. The 10-dB bandwidth and attenuation of SP-six-circle EBG structure are 4.98 GHz and 34.24 dB, respectively, while its ripple level in the lower passband is 2.77 dB and that in the higher passband is 6.55 dB. This structure although performs well in terms of bandwidth, it is inferior in terms of ripple level. When the two single-plane EBG structures are superposed in a compact dual-plane configuration (as shown in Fig. 1), the proposed dual-plane C-EBG microstrip structure shows a bandwidth and an attenuation within the stopband that are much larger than those shown by the two single-plane EBG structures. With only six EBG cells, this proposed structure is able to achieve a 10-dB bandwidth of 7.91 GHz with a center frequency of 10 GHz. This is extremely difficult to realize by using any single-plane EBG structure (Fig. 4). As compared to the meander 1-D EBG microstrip structure proposed in [12], the C-EBG microstrip structure is able to obtain a comparable stopband performance within a much smaller circuit area. Although the C-EBG structure exhibits good stopband performance, it suffers in terms of its ripple level. In this structure, the ripple level increases to 3.97 dB in the lower passband and 8.80 dB in the higher passband.

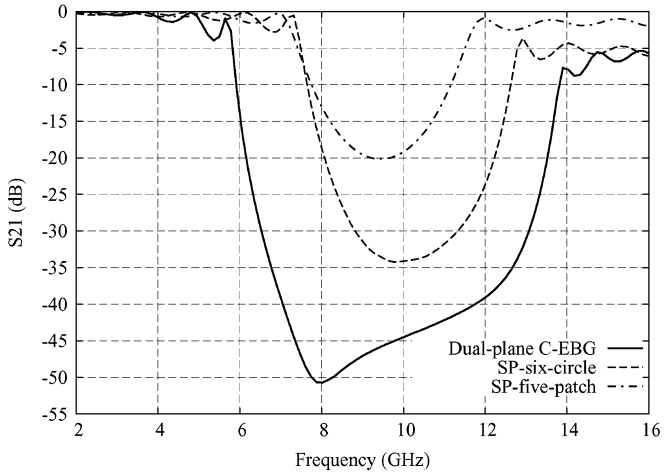

Fig. 4. Simulated S_{21} parameters of the dual-plane C-EBG structure and two single-plane EBG structures.

Like many other conventional methods to enhance a stopband in an EBG structure, the proposed dual-plane C-EBG structure introduces an increase in the bandwidth with high attenuation within the stopband at the expense of a high ripple level in the passband. Since the bandwidth and attenuation performance of the proposed structure is greatly enhanced, it allows a compromise in the stopband for a reduction in ripple level. As effective means to optimize the performance of an EBG structure in terms of its transmission in the passband, tapering techniques are to be used to tailor the high ripple level in the proposed C-EBG structure.

III. Tapering Techniques

Tapering techniques are effective for eliminating ripples in the passband caused by the periodicity in an EBG microstrip structure. In some tapered EBG microstrip structures, tapering techniques are applied by directly adopting tapering functions (such as Hamming tapering function [15] and Kaiser tapering function [16]) to modify the dimension of the periodic elements. The effects of adopting Bartlett, Hanning, Hamming, Nuttall, and Kaiser tapering function on the transmission of a 1-D planar EBG microstrip structure are compared and studied in [17]. The other approach to taper EBG structures is base on low sidelobe array theory [18] including Binomial array, Dolph–Tschebyscheff array (Chebyshev array), and Taylor

array. The significant effects of Binomial and Chebyshev distribution on the passband performance of an EBG microstrip structure have been shown by Karmakar *et al.* [19]. The effect of the Taylor distribution on the performance of a 1-D EBG coplanar waveguide (CPW) structure was shown in [20].

For a 1-D planar EBG microstrip structure with a single column of m circles etched in the ground plane of a microstrip line, the distribution of the dimension of the circle follows the following expression:

$$b_i = b_c \cdot T(z_i) \tag{7}$$

when tapering functions are applied, and

$$b_i = b_c \cdot a_i \tag{8}$$

when low sidelobe array theory is applied. i is an integer with a range from 1 to $m/2$ in the case that m is an even number and from 1 to $(m+1)/2$ in the case that m is an odd number. b_i is the radius (or the area) of the ith circle, b_c is the radius (or the area) of the central circle. In (7), $T(z)$ is the tapering function, and z_i is the normalized distance between the center of the ith circle and the center point of the structure that can be determined by the following expression:

$$z_i = \frac{2d_i}{L_t} \tag{9}$$

where d_i is the distance between the center of the ith circle and the center point of the microstrip line and L_t is the total length of the EBG microstrip structure. In (8), a_i is the ith coefficient in the array. In the case that m is even, the central circle does not exist but it is used to determine the dimension of the circle when employing tapering functions. Whereas when the low sidelobe array theory is applied, the two circles at the center are regarded as central circles in the calculation [9].

Table II shows some popular tapering functions used in EBG technology and their plots. In the Kaiser tapering function, $I_0(x)$ is the modified Bessel function of the first kind. The variance σ^2 in the Gaussian tapering function is generally set to 1 for a normal distribution. According to the definition, the value of the function varies in the range from 0 to 1 corresponding to $x \in [-1, 1]$ with the exception in Kaiser tapering function where $x \in [-(1/2), (1/2)]$.

The coefficients of a Binomial array are determined by the series binomial expansion of the function $(1+x)^{m-1}$ as

$$(1+x)^{m-1} = 1 + (m-1)x + \frac{(m-1)(m-2)}{2!}x^2 + \frac{(m-1)(m-2)(m-3)}{3!}x^3 + \cdots \tag{10}$$

The positive coefficients of the series expansion for a value of m can be used for tapering in a m-element 1-D EBG microstrip structure. The Binomial array has wide variations between the coefficients, especially for an array with a large number of elements. Chebyshev array is a compromise between uniform and Binomial array. Its coefficients are related to Tschebyscheff polynomial that satisfies the recurrence relations expressed as follows:

$$T_m(z) = z \cdot T_{m-1}(z) - \sqrt{(1-z^2)\{1-[T_{m-1}(z)]^2\}} \tag{11}$$

$$T_m(z) = 2z \cdot T_{m-1}(z) - T_{m-2}(z) \tag{12}$$

TABLE II
TAPERING FUNCTIONS

Type	Tapering Function $x \in [-1,1];\ y \in [0,1];\ a = 1$	Plot
Bartlett	$1 - \frac{\lvert x \rvert}{a}$	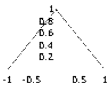
Connes	$(1 - \frac{x^2}{a^2})^2$	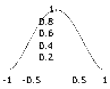
Hamming	$Hm_A(x) = 0.54 + 0.46\cos(\frac{\pi x}{a})$	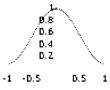
Hanning	$Hn_A(x) = \cos^2(\frac{\pi x}{2a}) = \frac{1}{2}(1+\cos(\frac{\pi x}{a}))$	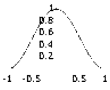
Cosine	$\cos(\frac{\pi x}{2a})$	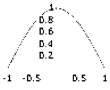
Welch	$1 - \frac{x^2}{a^2}$	
Kaiser	$\frac{I_0(4\sqrt{1-(2x)^2})}{I_0(4)}$ $x \in [-\frac{1}{2}, \frac{1}{2}]$	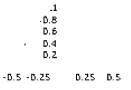
Blackman	$B_A(x) = 0.42 + 0.5\cos(\frac{\pi x}{a}) + 0.08\cos(\frac{2\pi x}{a})$	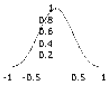
Gaussian	$e^{-x^2/(2\sigma^2)}$	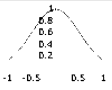

where $T_1(z) = 1$. Letting $z \equiv \cos\theta, T_m(z)$ is expressed as

$$T_m(z) = \cos(m \cdot \theta) = \cos[m \cdot \arccos(z)]. \tag{13}$$

The tapering techniques mentioned above are applied to the six-cell single-plane EBG microstrip structure with circles etched in the ground plane of a microstrip line that is one of the two single-plane EBG structures used to construct the proposed C-EBG structure (Fig. 1). Their effects on the performance of the EBG structure are studied. Taconic ($\varepsilon_r = 2.43, h = 30$ mils) is used as the substrate material of the structure. The center frequency of the stopband is 10 GHz giving a period of the structure $a_1 = 10.35$ mm, according to the Bragg reflection condition. The width of the microstrip w is 2.29 mm corresponding to a characteristics impedance of 50 Ω at 10 GHz. z_i is determined to be [0.182, 0.545, 0.909] for the tapering functions. To determine the coefficients in Binomial and Chebyshev array, the element number is set to six. For Chebyshev array, the major-to-minor lobe ratio is fixed at 25 dB. Table III shows the corresponding values of every tapering function and the normalized coefficients of the arrays.

TABLE III
VALUE OF TAPERING FUNCTIONS AND NORMALIZED COFFICIENTS

Type	$T(z_1)$	$T(z_2)$	$T(z_3)$
Bartlett	0.82	0.46	0.09
Blackman	0.87	0.27	0.01
Connes	0.94	0.49	0.03
Cosine	0.96	0.66	0.14
Gaussian	0.98	0.86	0.66
Hamming	0.93	0.48	0.10
Hanning	0.92	0.43	0.02
Welch	0.97	0.70	0.17
Kaiser	0.94	0.58	0.16
Type	a_1	a_2	a_3
Binomial	1	0.50	0.10
Chebyshev	1	0.73	0.39

The area of the circle is tapered according to (7) or (8) where the filling factor (r/a_1) of the central circle is set to be 0.25.

All tapered EBG structures are simulated. Each tapered EBG structure exhibits a stopband centered at 10 GHz although the bandwidth and attenuation within the stopband, and the ripple level in the passband vary from one to another. Some structures show similar transmission characteristics, thus, they are classified together to form two groups. Table IV shows the performances of structures in these two groups in terms of bandwidth and attenuation of the stopband, ripple levels in the passbands, and sidelobe levels in the S_{11} parameter. As can be seen in the table, structures in Group One are good in terms of ripple level performance but poor in terms of stopband performance. The stopband performances of the structures in Group Two are better than those in Group One but the ripple levels are higher in the Cosine and Welch tapered EBG structure. The Kaiser tapered EBG structure in Group Two has the lowest ripple level of 0.08 dB in the lower passband and 2.4 dB in the higher passband. Therefore, it is able to tolerate an increase in the ripple level for an enhancement of the stopband. The superior transmission in the passband of the Kaiser tapered EBG structure is indicated by its low sidelobe levels of the S_{11} parameter in Fig. 5.

Fig. 6 shows the simulated S_{21} parameters of the tapered 1-D EBG microstrip structures (the Blackman, Binomial, Kaiser, Chebyshev, and Gaussian tapered EBG structure) and that of the EBG structure with a uniform distribution. Binomial and Kaiser tapered EBG structure are chosen as representatives of their groups. As shown in the figure, the structure with a uniform distribution displays a good bandwidth performance while exhibiting high ripple levels in both passbands. As can be seen, all tapered structures have a significant reduction in the ripple level in both passbands. However, this comes at the expense of a reduction in both the bandwidth and attenuation within the stopband. In all tapered structures, the Gaussian tapered EBG structure behaves the most similarly to the structure with a uniform distribution. The Blackman tapered EBG structure has the lowest ripple levels (0.16 dB in the lower passband and 1.9 dB in the higher passband). However, its bandwidth and attenuation are greatly reduced.

It is observed that for the performance of tapered EBG structures, the reduction in the ripple level in the passband is commonly proportional to the reduction in the bandwidth and attenuation of the stopband. Nevertheless, the Chebyshev tapered EBG structure exhibits a 4.3-GHz-wide stopband at 10 dB with an attenuation of 24.36 dB, a ripple level of 0.17 dB in the lower passband, and a ripple level of 2.9 dB in the higher passband. This is similar to the performance of the Kaiser tapered EBG structure in the sense that they are both able to obtain a low ripple level while maintaining a relatively wide and deep stopband. Although their stopband performances are not the best, the very low ripple level in the passband enables them to obtain a good tradeoff between the ripple level in the passband, and the bandwidth and attenuation of the stopband. As compared to Kaiser tapered EBG structure, the Chebyshev tapered EBG structure has higher ripple levels in both passbands, but smaller transition width from the passband to the stopband that implies a higher selectivity [19].

IV. TAPERED DUAL-PLANE C-EBG MICROSTRIP FILTER STRUCTURE

A. Design and Numerical Simulation

To eliminate the ripple in the passband due to the periodicity in the dual-plane C-EBG structure proposed in Fig. 1, the Chebyshev distribution is adopted to taper the dimension of the EBG unit and two tapered C-EBG structures are proposed; the ground-tapered C-EBG structure and the double-tapered C-EBG structure. Fig. 7 shows the schematic of the ground-tapered C-EBG structure where the area of the etched circles at two ends of the structure are tapered. The coefficients of the six-element Chebyshev array obtained previously (Table III) are used in the design. Amplitude 1 corresponds to the area of the two central circles with a filling factor (r/a_1) of 0.25. Accordingly, the radius of the circle from the left to the right is 1.61, 2.21, 2.59, 2.59, 2.21, and 1.61 mm, respectively.

Fig. 8 shows the schematic of the double-tapered C-EBG structure in which the dimensions of the EBG units in both the ground plane and the microstrip line are tapered by applying the Chebyshev distribution. Besides the six-element Chebyshev array that is applied to tailor the dimension of the etched circle in the ground plane, the coefficients of the five-element Chebyshev array are used to taper the area of the square patch in the microstrip line. With a major-to-minor lobe ratio set to be 25 dB, its normalized coefficients are determined to be 1, 0.797, and 0.393. l_a and w_a of the central patch are both set to 5 mm. Accordingly, l_{a2}, w_{a2}, l_{a3}, and w_{a3} can be determined to be 4.46, 4.46, 3.13, and 3.13 mm, respectively.

Fig. 9 shows the simulated S-parameters for the ground-tapered C-EBG structure (Fig. 7), the double-tapered C-EBG structure (Fig. 8), and the proposed uniform C-EBG structure (Fig. 1). As can be seen in Fig. 1(a), the uniform C-EBG structure shows a 25-dB bandwidth of 7.00 GHz with an attenuation of 50.71 dB. The ground-tapered C-EBG structure has a 25-dB bandwidth of 6.05 GHz with an attenuation of 67.71 dB. This is a reduction of about 14% of bandwidth shown by the uniform C-EBG structure. However, as compared to the uniform C-EBG structure, the ground-tapered C-EBG structure has a ripple level that is significantly lowered from 3.97 to 0.92 dB in the lower passband and from 8.80 to 3.42 dB in the higher passband. For the ground-tapered C-EBG structure, its stopband performance

TABLE IV
PERFORMANCE OF TAPERED 1-D EBG MICROSTRIP STRUCTURES

Group	Tapering Techniques	Bandwidth (GHz)	Attenuation (dB)	Ripple Level		Side Lobe Level	
				Lower	Higher	Lower	Higher
Group One	Hanning, Connes, Binomial Hamming, Bartlett	$3.8 \sim 4.0$	$15 \sim 17$	$0.08 \sim 0.16$ dB	$2.3 \sim 2.9$ dB	> 21 dB	> 8 dB
Group Two	Kaiser Cosine, Welch	$4.0 \sim 4.3$	$19 \sim 21$	$0.21 \sim 0.31$ dB (except Kaiser)	$3.0 \sim 3.5$ dB (except Kaiser)	> 15 dB (except Kaiser)	> 9 dB (except Kaiser)

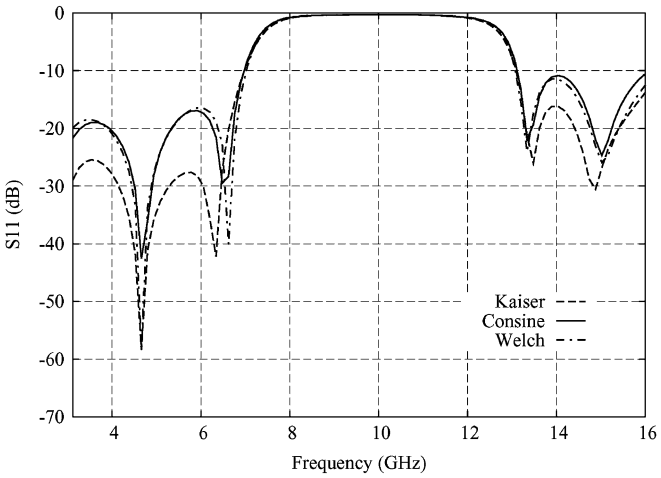

Fig. 5. Simulated S_{11} parameters of tapered 1-D EBG microstrip structures in Group Two.

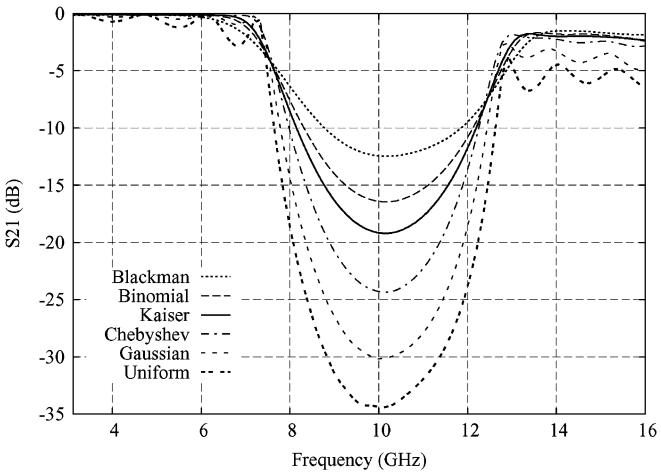

Fig. 6. Simulated S_{21} parameters of tapered 1-D EBG microstrip structures and the EBG structure with a uniform distribution.

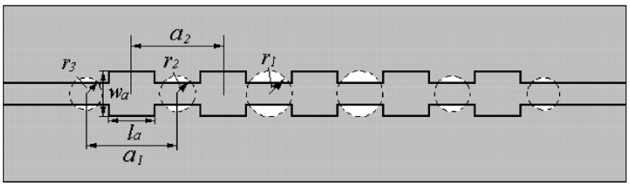

Fig. 7. Schematic of the ground-tapered C-EBG structure adopting the Chebyshev distribution.

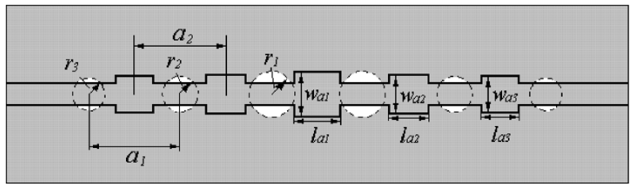

Fig. 8. Schematic of the ground-tapered C-EBG structure adopting the Chebyshev distribution.

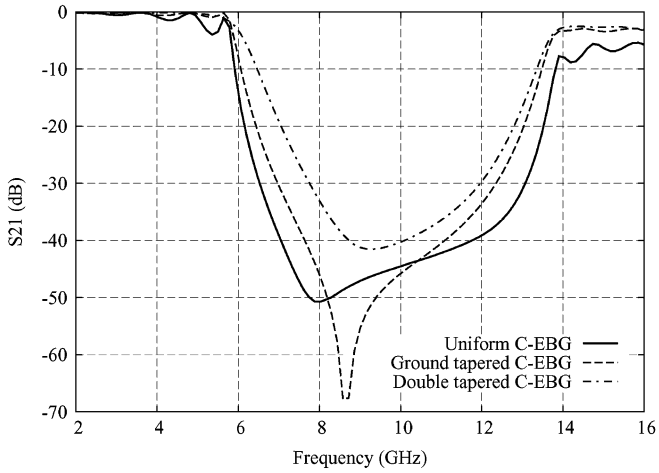

(*a*)

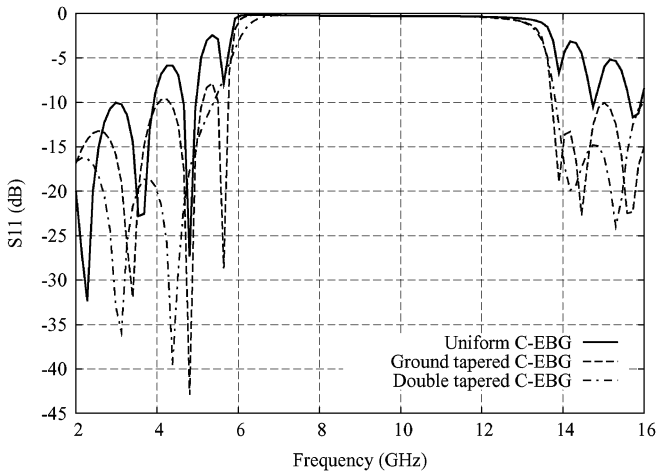

(*b*)

Fig. 9. Simulated S-parameters of the tapered and uniform dual-plane C-EBG microstrip structure. (a) S_{21}. (b) S_{11}.

is slightly degraded by the adopted tapering technique. However, its ripple level is significantly lowered, which implies an excellent transmission in the passband.

In the same figure, the double-tapered C-EBG structure exhibits a stopband with a 25-dB bandwidth of 5.05 dB and an attenuation of 41.54 dB. Its ripple level in the lower passband is

0.16 dB whereas that in the higher passband is 3.20 dB. Comparing the double-tapered C-EBG structure to the ground-tapered C-EBG structure, its performance is improved in terms of ripple levels in both passbands. However, the bandwidth and attenuation of its stopband are reduced. Although the stopband performances of both tapered C-EBG structures are degraded, their bandwidth and attenuation are still larger than those in the single-plane EBG structures (Fig. 4). Fig. 9(b) shows their S_{11} parameters. It is observed that both tapered C-EBG structures show much lower sidelobe levels than those of the uniform structure, which implies the smooth transmission in the passband. The double-tapered C-EBG structure has the best performance of the three structures in terms of ripple level in the passband while its stopband performance is the worst.

As revealed by the results above, the ripple level of the proposed C-EBG structure can be tailored by applying a tapering technique to taper the dimension of EBG units on different planes, which comes with degradation of the stopband performance. A double-tapered C-EBG structure is able to obtain a lower ripple level than that shown in a single tapered C-EBG structure such as the ground-tapered C-EBG structure. With the unique dual-plane configuration, the filtering functionality of the proposed C-EBG structure can be adjusted to meet different requirements in various applications.

B. Measurement Results

Both the proposed ground-tapered and double-tapered five-patch six-circle dual-plane C-EBG microstrip structure were fabricated and tested. Fig. 10(a) and (b) shows the modulated microstrip line and the ground plane with etched circles of the fabricated structures, respectively. These structures are highly compact with a dimension of 70 mm by 26 mm as shown in Fig. 10. Figs. 11 and 12, show the simulated and measured S-parameters of the fabricated ground-tapered C-EBG structure and double-tapered C-EBG structure, respectively. As can be seen from the measurement results in the two figures, with only six EBG cells, the ground-tapered C-EBG structure is able to achieve a 25-dB bandwidth of 5.98 GHz at 10 GHz, with an attenuation of 39.00 dB, a ripple level of 1.56 dB in the lower passband, and a ripple level of 4.68 dB in the higher passband whereas the fabricated double-tapered C-EBG structure exhibits a 25-dB bandwidth of 4.87 GHz, an attenuation of 52.9 dB, a ripple level of 0.51 dB in the lower passband, and a ripple level of 5.47 dB in the higher passband. An excellent agreement between the measurement and the simulation results have been obtained in both the proposed tapered dual-plane C-EBG structures. The slight difference is probably due to the effect of SMA connectors, the lack of material uniformity and cell uniformity, the over etching, and the nonideal soldering. The infinite ground plane assumed in the simulation is another possible cause for the difference.

Both proposed tapered dual-plane C-EBG structures demonstrate the advantages of large bandwidth, high attenuation, smooth passband, compact size, and easy fabrication process. The ground-tapered C-EBG structure is able to obtain an ultra-wide stopband with very high attenuation and relatively small ripple levels in both passbands whereas the double-tapered C-EBG structure shows an extremely small ripple level in the passband but a relatively smaller stopband bandwidth and attenuation. Due to their common characteristics and the unique feature of each structure, these two proposed structures can be

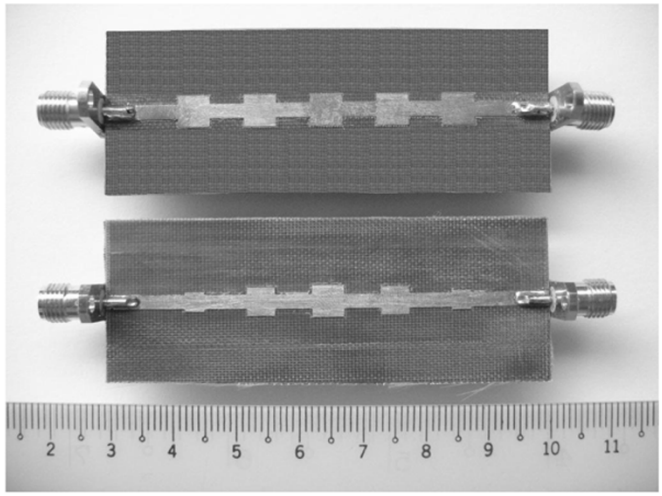

Fig. 10. Photographs of the fabricated ground-tapered dual-plane C-EBG microstrip structure (upper) and the fabricated double-tapered dual-plane C-EBG microstrip structure (lower). (a) Microstrip line. (b) Ground plane.

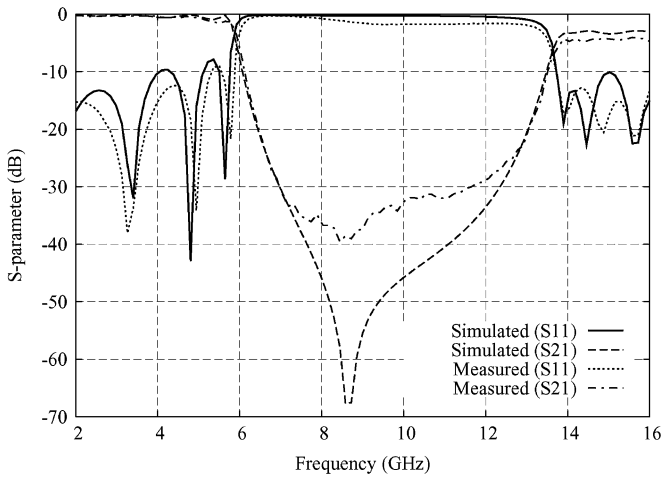

Fig. 11. Simulated and measured S-parameters of the ground-tapered C-EBG microstrip structure.

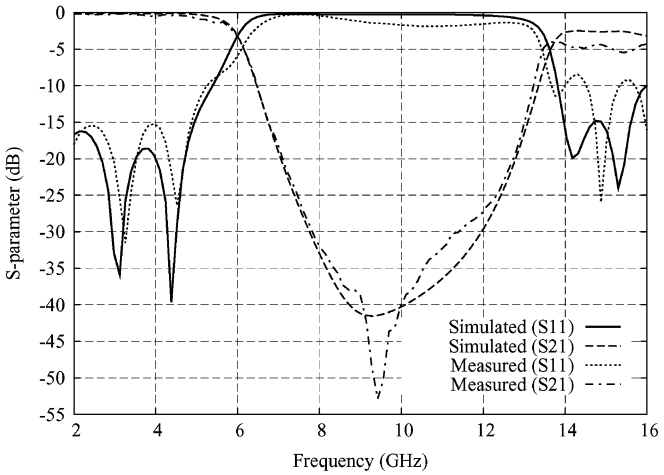

Fig. 12. Simulated and measured S-parameters of the double-tapered C-EBG microstrip structure.

easily applied to various circuit applications to meet different requirements on the passband and the stopband performance.

V. Conclusion

In this paper, the design and implementation of two novel tapered dual-plane C-EBG microstrip filter structures have been presented. Due to the unique dual-plane arrangement, the novel structure has an ultrawide stopband with a large bandwidth of above 4.8 GHz at 25 dB and high attenuation of beyond 35 dB within a compact physical size. Its ripple level in the passband is well tailored by adopting the Chebyshev distribution, and therefore, the tapered C-EBG structure exhibits an excellent transmission in the passband. The proposed structure is easy to fabricate and is compatible with MMIC technology. Both tapered C-EBG structures were fabricated and tested. The measurement results are in good agreement with the simulation results. The novel design of this structure is able to achieve high performance as a bandstop filter with superior passband and stopband characteristics. The proposed 1-D EBG dual-plane configuration can be further employed in other applications for compact microwave circuits. For example, it can be used as the reflectors in the design of resonators or for the coupling elimination of two close microstrip lines.

Acknowledgment

The authors would like to thank the anonymous reviewers for their valuable suggestions.

References

[1] E. Yablonovitch, "Inhibited spontaneous emission in solid-state physics and electronics," *Phys. Rev. Lett.*, vol. 58, no. 20, pp. 2059–2062, May 1987.

[2] S. John, "Strong localization of photons in certain disordered dielectric superlattices," *Phys. Rev. Lett.*, vol. 58, no. 23, pp. 2486–2489, Jun. 1987.

[3] G. Kurizki and A. Z. Genack, "Suppression of molecular interactions in periodic dielectric structures," *Phys. Rev. Lett.*, vol. 61, no. 19, pp. 2269–2271, Nov. 1988.

[4] E. R. Brown, C. D. Parker, and E. Yablonovitch, "Radiation properties of a planar antenna on a photonic-crystal substrate," *J. Opt. Soc. Amer. B*, vol. 10, no. 2, pp. 404–407, Feb. 1993.

[5] R. Gonzalo, P. D. Maagt, and M. Sorolla, "Enhanced patch-antenna performance by suppressing surface waves using photonic-bandgap substrates," *IEEE Trans. Microw. Theory Techn.*, vol. 47, no. 11, pp. 2131–2138, Nov. 1999.

[6] V. Radisic, Y. Qian, and T. Itoh, "Broad-band power amplifier using dielectric photonic bandgap structure," *IEEE Microw. Guided Wave Lett.*, vol. 8, no. 1, pp. 13–14, Jan. 1998.

[7] V. Radisic, Y. Qian, R. Coccioli, and T. Itoh, "Novel 2-D photonic bandgap structure for microstrip lines," *IEEE Microw. Guided Wave Lett.*, vol. 8, no. 2, pp. 69–71, Feb. 1998.

[8] F. Falcone, T. Lopetegi, and M. Sorolla, "1-D and 2-D photonic bandgap microstrip structures," *Microw. Opt. Technol. Lett.*, vol. 22, no. 6, pp. 411–412, Sep. 1999.

[9] Q. Xue, K. M. Shum, and C. H. Chan, "Novel 1-D microstrip PBG cells," *IEEE Microw. Guided Wave Lett.*, vol. 10, no. 10, pp. 403–405, Oct. 2000.

[10] T. Lopetegi, M. A. G. Laso, J. Hernandez, M. Bacaicoa, D. Benito, M. J. Garde, M. Sorolla, and M. Guglielmi, "New microstrip 'wiggly-line' filters with spurious passband suppression," *IEEE Trans. Microw. Theory Techn.*, vol. 49, no. 9, pp. 1593–1598, Sep. 2001.

[11] D. Ahn, J. Park, C. Kim, J. Kim, Y. Qian, and T. Itoh, "A design of the low-pass filter using the novel microstrip defected ground structure," *IEEE Trans. Microw. Theory Techn.*, vol. 49, no. 1, pp. 86–93, Jan. 2001.

[12] F. Falcone, T. Lopetegi, M. Irisarri, M. A. G. Laso, M. J. Erro, and M. Sorolla, "Compact photonic bandgap microstrip structures," *Microw. Opt. Technol. Lett.*, vol. 23, no. 4, pp. 233–236, Nov. 1999.

[13] J. Kim and H. Lee, "Wideband and compact bandstop filter structure using double-plane superposition," *IEEE Microw. Wireless Compon. Lett.*, vol. 13, no. 7, pp. 279–280, Jul. 2003.

[14] S. Y. Huang, Y. H. Lee, and Y. Lu, "A novel compact electromagnetic bandgap filter design," presented at the 2004 Asia-Pacific Microwave Conf., New Delhi, India, Dec. 2004.

[15] A. D'Orazio, M. D. Sario, V. Gadaleta, V. Petruzzelli, and F. Prudenzano, "Meander microstrip photonic bandgap filter using a Kaiser tapering window," *Electron. Lett.*, vol. 37, no. 19, pp. 1165–1167, Sep. 2001.

[16] T. Lopetegi, M. A. G. Laso, M. Irisarri, M. J. Erro, F. Falcone, and M. Sorolla, "Optimization of compact photonic bandgap microstrip structures," *Microw. Opt. Technol. Lett.*, vol. 26, no. 4, pp. 211–216, Aug. 2000.

[17] M. Bozzetti, A. D'Orazio, M. D. Sario, V. Petruzzelli, F. Prudenzano, and F. Renna, "Tapered photonic bandgap microstrip lowpass filters: Design and realization," *Proc. IEE Microwaves, Antennas and Propagation*, vol. 150, no. 6, pp. 459–462, Dec. 2003.

[18] C. Balanis, *Antenna Theory Analysis and Design*. New York: Wiley, 1997, 2nd, pp. 294–299.

[19] N. C. Karmakar and M. N. Mollah, "Investigations into nonuniform photonic-bandgap microstripline low-pass filters," *IEEE Trans. Microw. Theory Techn.*, vol. 51, no. 2, pp. 564–572, Feb. 2003.

[20] S. K. Padhi, "Improved performance of EBG's on a co-planar transmission line using tapered distribution," *Microw. Opt. Technol. Lett.*, vol. 42, no. 2, pp. 128–131, Jul. 2004.

Shao Ying Huang (S'04) received the B.Eng. degree from Nanyang Technological University, Singapore, in 2002, where she is currently working toward the M.Eng. degree in the School of Electrical and Electronic Engineering.

Her research interest includes the design, development, and modeling of electromagnetic bandgap structures and their applications.

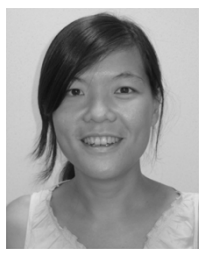

Yee Hui Lee (S'96–M'02) received the B.Eng. and M.Eng. degree from the Nanyang Technological University, Singapore, in 1996 and 1998, respectively. She received her Ph.D. degree from the University of York, York, U.K., in 2002.

Since July 2002, she has been an Assistant Professor at the School of Electrical and Electronic Engineering, Nanyang Technological University. Her interest is in evolutionary techniques, computational electromagnetics, and antenna design.